



# Effect of printing parameters and post-process on surface roughness and dimensional deviation of PLA parts fabricated by extrusion-based 3D printing

Emre Taşcıoğlu<sup>1</sup> · Özhan Kıtay<sup>2</sup> · Ali Özkan Keskin<sup>1</sup> · Yusuf Kaynak<sup>3</sup>

Received: 28 July 2021 / Accepted: 14 February 2022 / Published online: 16 March 2022

© The Author(s), under exclusive licence to The Brazilian Society of Mechanical Sciences and Engineering 2022

## Abstract

One of the commonly used additive manufacturing methods is extrusion-based 3D printing (e.g., fused filament fabrication or FFF) that is generally required post-processing to make fabricated components ready to be used. This paper considers two major points to assess the surface enhancement of components made of polylactic acid (PLA) material. One is the role of processing parameters including layer thickness, print speed, and printing temperature on dimensional and surface quality of fabricated parts. The second one is post-processing and its parameters. Vibratory surface finishing (VSF) is used as post-processing operation, and treatment time is varied to observe its effect on the surface and dimensional variation of the fabricated parts. The effect of input variables on measured outputs is also presented by using statistical approaches including regression and analysis of variance. This study reveals that layer thickness is dominating parameter to control surface and dimensional quality of both as-printed and post-treated samples. However, printing temperature also plays a notable role on the dimensional accuracy of specimens. Considering post-processing, while it is notable, duration is the key factor determining the final surface quality of fabricated samples. The surface roughness of as-printed samples was reduced by 66% through post-processing operation.

**Keywords** Additive manufacturing · Material extrusion · Post-processing · Polylactic acid · Surface quality

## 1 Introduction

Additive manufacturing (AM) is a production method that enables rapid prototype production as well as facilitating the production of complex-shaped parts that cannot be produced with traditional manufacturing methods. There are many additive manufacturing methods with different working

principles [1], and these methods are gathered under the ISO/ASTM 52900:15 standard [2]. Among these, one of the most suitable for rapid prototyping in terms of short production time, maintenance and material price, easy material change, variety of material, the low-temperature operation is the material extrusion additive manufacturing (AM) that is also known as Fused Filament Fabrication (FFF), or Fused Deposition Modeling (FDM) method, which works with the material extrusion principle [3].

Many different polymer-based materials and even binder metals and ceramic can be used with material extrusion. The main polymer materials commonly used are acrylonitrile butadiene styrene (ABS) terpolymer and polylactic acid (PLA) [4]. The lower thermal expansion (89  $\mu\text{m}/\text{m}^\circ\text{C}$  for ABS and 80  $\mu\text{m}/\text{m}^\circ\text{C}$  for PLA [5]) and higher mechanical properties (Tensile strength of PLA: 51 MPa while ABS has 41 MPa tensile strength [6]) are the superior aspects of PLA compared to ABS, and this situation improves the printability of PLA [7]. It is widely used in drug, textile, and electronics fields, also especially in biomedical applications as it is also a biocompatible polymer material [8]. Especially in

Technical Editor: Zilda de Castro Silveira.

✉ Yusuf Kaynak  
yusuf.kaynak@marmara.edu.tr

<sup>1</sup> R&D Center, Torun Bakır Alaşımaları Metal Sanayi ve Ticaret A.Ş., GOSB İhsan Dede Cad. No:116, Gebze 41480, Kocaeli, Turkey

<sup>2</sup> Department of Machine and Metal Technologies, Bilecik Seyh Edebali University, Gülümbe Campus, 11230 Bilecik, Turkey

<sup>3</sup> Department of Mechanical Engineering, Marmara University, Recep Tayyip Erdoğan Külliyesi, Aydınevler Mah. İdealtepe Yolu, No:15, 34854 Istanbul, Turkey

the automobile industry, the proportion of components such as air filter and interior trim, spare tire cover, car floor mat, dashboard, etc., produced from PLA material [9].

Fabricating components through material extrusion is of great advantages as compared with conventional manufacturing. Geometries with a small size, lattice structure or complex shape that cannot be produced with traditional methods and with the least material used with topology optimization can be produced by the material extrusion AM method [10]. But, produced parts should also meet some certain requirements in terms of dimensional accuracy and surface roughness. It should be noted that dimensional accuracy and surface roughness are functions of process and product design parameters [4]. Although, it has many advantages, the poor surface quality of the parts produced by material extrusion AM remains as an important problem that needs to be handled.

There are various studies in the literature to improve the surface quality of parts produced with material extrusion AM by utilizing pre-processing and post-processing [11]. Processing parameters including layer thickness, printing temperature, raster angle, and built orientation of part are optimized to enhance the surface quality of parts produced through material extrusion in pre-processing [1, 12, 13]. Kovan et al. [12] reported that keeping the layer thickness low results in reducing the surface roughness, while the effect of nozzle temperature on the roughness is limited. Wankhede et al. [14] reported that the layer thickness should be chosen low for the best surface roughness value in their study where they applied the Taguchi method. There are many studies investigating the effect of built orientation angle on surface quality [15], and Pugalendhi et al. [16] showed that  $0^\circ$  and  $90^\circ$  are optimum values for surface quality. Rayegani and Onwubolu [17] examined the effects of both built orientation and raster angle on tensile strength and stated that  $0^\circ$  built orientation gives optimum results. Although the surface roughness values and mechanical properties can be partially improved by altering process parameters, the surface quality remains far from the desired level. Therefore, post-processing is needed. As material extrusion AM is not comparable with the surface quality of parts that are fabricated by using other AM methods [18]. As a result of many different chemicals [3] and mechanical [11] post-processing applications, values close to the desired surface qualities were obtained. However, this time, inconsistencies in the dimensional accuracy of the parts produced by the material extrusion AM process with a certain dimensional deviation from the CAD model dimensions seem to be inevitable.

Chemical and mechanical processing is not fully automatized as yet. In most cases, post-processing is employed by one through dedicated person. This leads to long post-processing time and relatively increased manufacturing cost.

Alternative approaches should be developed to help post-process to be automatized and reduced cost. In the meantime, from industrial point of view, repeatable and reliable processes are required to be able to produce components that have predictable surface aspects. Vibratory surface finishing (VSF) is a post-processing method that fits this description. In the literature, barrel finishing (BF) method has been mainly used in surface improvement studies of material extrusion AM parts [19, 20]. However, BF has the principle of working with vertical vibration while VSF with horizontal vibration, hence they are actually different [21]. In the surface improvement works with VSF, polymer materials produced by selective laser sintering (SLS) method were preferred [22, 23]. However, SLS and material extrusion AM are methods with different working principles. Study focused on implementing VSF to polymer materials presented the effect of the process duration as well as the shape and size of the abrasive particle on surface was examined [24]. Therefore, there are not yet studies examining the surface quality of PLA materials, especially the combination of both material extrusion AM process parameters and VSF process.

Considering all these challenges and expectation, this current paper proposes vibratory surface finishing operation for enhancing surface aspects of components fabricated by material extrusion operations. Thus, this study focuses on the influence of process parameters and vibratory surface finishing operation on surface aspects and dimensional accuracy of PLA samples.

## 2 Experimental setup

The feedstock filament material with diameter of 2.85 mm used in this study is Tough white polylactic acid (PLA) produced by ULTIMAKER [25]. Its melting point is  $145\text{--}160^\circ\text{C}$ . It has an elongation of 5.2% at break and Shore D hardness of 83. ULTIMAKER S5 Pro 3D [26] printing machine is used to fabricate rectangular prism (20 mm x 20 mm x 15mm) samples as shown in Fig. 1. Built volume in printer specifications is  $330 \times 240 \times 300$  mm, and XYZ resolution is 6.9, 6.9, 2.5 micron. In the fixed parameters, wall thickness is 1 mm, build plate temperature is  $60^\circ\text{C}$ , and line width is 0.35 mm. Nozzle diameter is 0.4 mm, and generally recommended layer thickness is approximately half the nozzle diameter [27]. The values of 0.16 and 0.24 mm used in the study are in accordance with this recommendation. In addition, layer thickness of 0.08 mm was also used. Triangles pattern strategy was used to build these samples with infill density of 40% and 50 Hz excitation frequency. It should be noted that preferred infill density meets the requirements for many applications in industry.

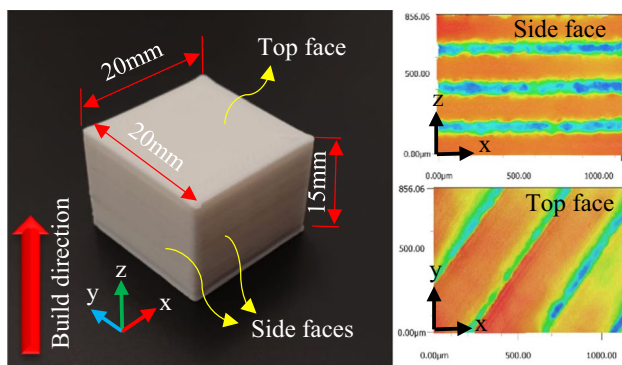


**Fig. 1** Geometry and size of samples fabricated and used in this study

This fill pattern is widely used in the material extrusion AM method as it has an advantage in mechanical strength when a tension is applied perpendicular to one side of the printed part [28]. Therefore, this method is preferred. Two samples from each condition and 48 samples in total were produced. Extrusion-based 3D printing parameters used in this study are shown in Table 1. Extrusion-based 3D printing scheme is shown in Fig. 2. The slicer software used is Ultimaker Cura version 4.8.

To enhance the surface of these material extrusion AM manufactured samples, post-processing namely vibratory surface finish (VSF) is employed. The vibratory surface finishing process was performed by using the ETP-100 ERBA VSF machine having a 0.55 KW driving power and 1400 rpm. A photograph of vibratory surface finishing machine is shown in Fig. 3a. For the VSF operation, media pellets used in this study were ceramic abrasive of size  $25 \times 25$  mm with angle cut shape media. VSF operation is performed under water-wet condition. It should be noted that four different durations (1, 2, 3 and 4 h) for the VSF operation were considered. At the end of each VSF period, dimensional accuracy values were measured with a DEA SM25 Scan Head CMM device as shown in Fig. 3b. Keyence digital optical microscopy was utilized to measure surface roughness and the surface topography. Its resolution is  $0.005 \mu\text{m}$ . Three measurements were made for each sample.

**Table 1** Material extrusion AM and VSF process parameters

Material	Layer thickness (mm)	Print speed (mm/s)	Printing temperature ( $^{\circ}\text{C}$ )	VSF post-treatment durations (h)
Tough PLA (White)	0.08	50	190	1, 2, 3, 4
	0.16		205	
	0.24		220	

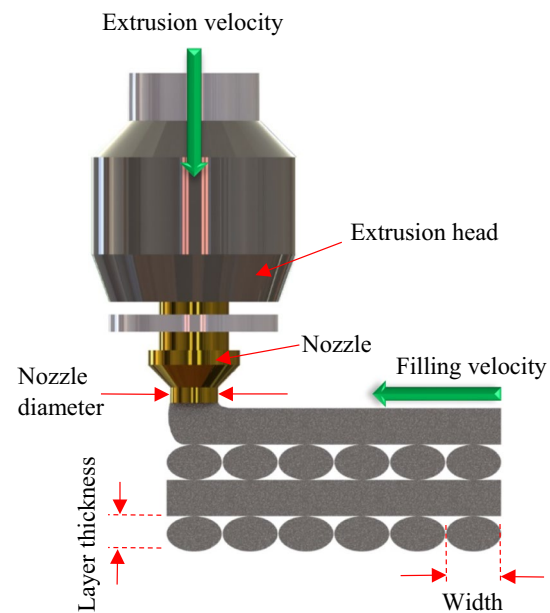


**Fig. 2** Schematic representation of the extrusion parameters

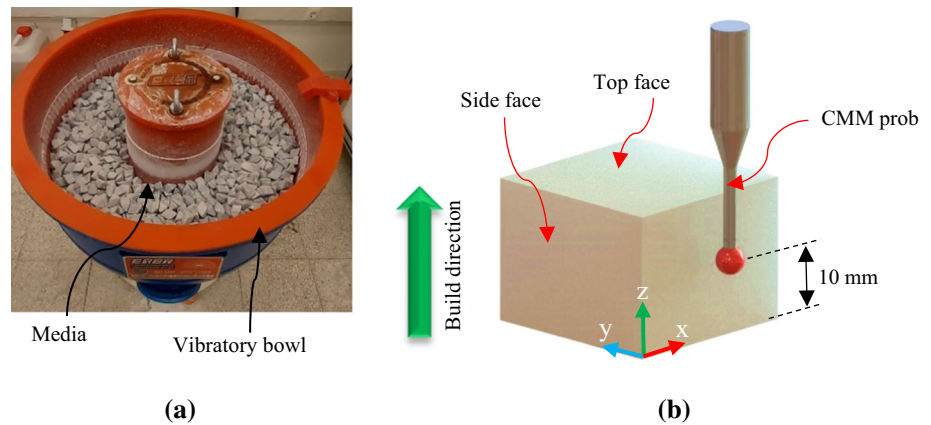
## 3 Results and discussion

### 3.1 Surface roughness and topography

Surface roughness and topography are key parameters indicating the precision of material extrusion process, and these also affect the functionality of components fabricated by material extrusion. However, it is known fact that arithmetical average surface roughness ( $R_a$ ) of samples fabricated by material extrusion varies in between 9 and  $40 \mu\text{m}$  [18] that can be categorize as poor surface roughness. Therefore, it is important to examine the surface qualities of as-printed parts. Figure 4 shows measured surface roughness and corresponding topographies for built and scanning area of the samples fabricated by materials extrusion. There are large variation in surface roughness values with AM process parameters. The results obtained from the scanning area are more reasonable in terms of both surface roughness and topography. Layer thickness stands out as the main parameter affecting the surface quality. It should be noted that the effect of printing temperature remained almost negligible. It is obvious that the surface quality deteriorated as the layer thickness increased, and this is true for both scanning and built area.

Since the melting temperature of the material is  $160 \text{ }^{\circ}\text{C}$ , the viscous behavior of PLA is affected by the nozzle temperature. In addition to the extrusion process, of course, viscosity is an effective in the theoretical  $R_a$  values being different from the measured values. As a matter of fact, the cooling rate of PLA melted in larger layer thickness ( $hc$ )

**Fig. 3** (a) VSF machine, (b) schematic presentation of CMM process [27]



should be slower than in lower  $hc$ . This means that the existence of the viscous effect is longer.

Theoretical calculation of surface roughness values as a function of layer thickness is also presented in the literature by using the following equation [29].

$$Ra = \frac{1}{\sqrt{2hc}}(0.316hc)^2 \quad (1)$$

where  $hc$  indicates layer thickness or height [29]. This equation indicates that the higher the layer thickness, the larger the average surface roughness values of produced parts. The experimental results presented in this current work supports this by presenting the increased trend in roughness with increased layer thickness. By using this equation, calculated arithmetical surface roughness for three different layer thickness is calculated. As shown in Fig. 4, calculated surface roughness values of built area show very good agreement with the experimentally measured results as 13%, 2%, and 4% at 0.08, 0.16 and 0.24 mm of layer thickness, respectively. It is apparent that layer thickness plays a key role in determining the surface quality of fabricated parts [30] and easy to control by reducing the layer thickness, but it also directly affects the cost of process by changing building time [31].

For this reason, instead of increasing production time by altering process parameters to enhance surface quality of fabricated parts, post-processing should be utilized to have products with better surface quality. Indeed, Fig. 5 supports this argument. As surface topographies in between as-printed and post-processed samples compared, large improvements can be easily noticed. While the parallel cylindrical stripes on built area of as-printed samples are visible, they disappeared after post-treatment.

Quantitative measurements of roughness value from these surfaces confirm this as presented in Fig. 6. It shows the arithmetic average surface roughness of the as-printed samples' built area and comparison with the surface roughness

of the post-processed samples. Remarkable improvements on the surface of samples through post-processing is evidently achieved. It is clear that VSF finishing can make significant improvements in the surface quality of printed parts and post-processing duration determines the final surface roughness values for all samples subjected to post-processing. It is obvious from the figure that increasing post-processing time leads to producing much better surface quality. When samples fabricated through 0.24mm layer thickness are subjected to 4  $h$  post-processing, it is possible to reduce its surface roughness value from 17 to 6  $\mu\text{m}$ . This means that approximately 66% reduction in arithmetic surface roughness is achieved. When considering samples fabricated with smaller layer thickness, much smaller roughness can be obtained resulting from post-processing operations as shown in Fig. 6.

Employing post-processing is also helpful for improving quality of scan area, as shown in Fig. 7. In this case, layer thickness is also determining the final surface quality. Post-processing has limited effect on the samples with the largest layer thickness, 0.24 mm, tested in this work; however, the difference in between as-printed ones and post-processed ones in terms of surface roughness is notably large enough when layer thicknesses are 0.16 and 0.08 mm. 3-D surface topography depicted in Fig. 8 also supports the presented results in Fig. 7. While much smooth surface is generated with samples fabricated through smaller layer thickness, the parallel cylindrical stripes on the surface of post-processed samples produced with large layer thickness are still visible.

### 3.2 Dimensional deviation

The sudden heating and cooling during the material extrusion AM process results in the residual stresses in the internal structure of the produced part [7]. These stresses lead to occurring distortion and eventually cause the part to be produced with some deviations different from the nominal dimensions designed in the CAD drawing.

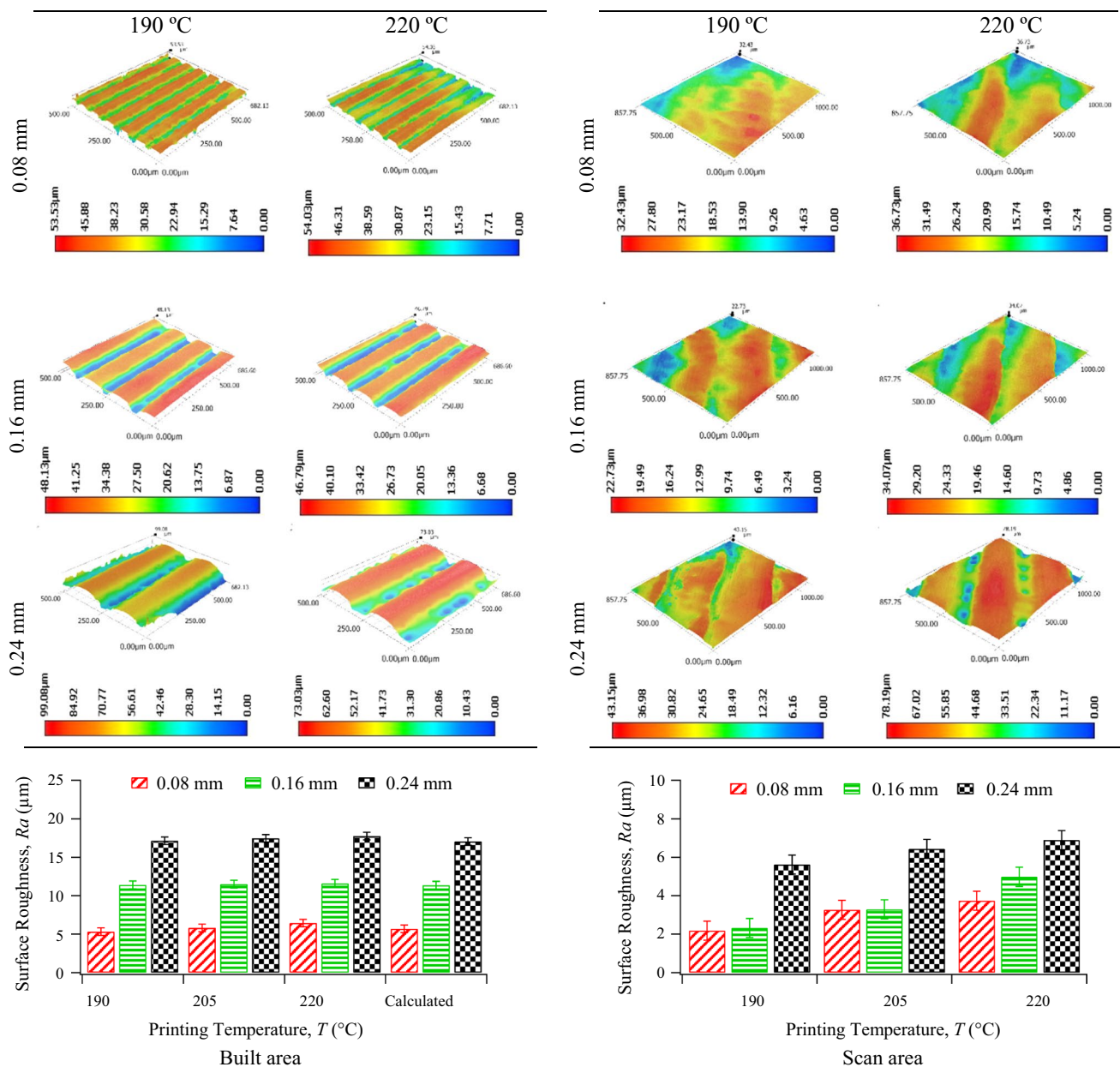


Fig. 4 Measured average surface roughness and topography of as-printed samples

Another reason for these dimensional deviations, as well as poor surface finishes, is the slicing and conversion of the CAD model to the STL format [32]. In cases where the improvements made with the material extrusion AM process parameters are insufficient, it is inevitable to resort to post-processing methods. As a matter of fact, considering the dimensional deviations in the part to be produced before post-processing, a dimensional positive offset can be considered on the outer surface [33]. However, due to the mentioned reasons, negative or positive shrinkage situations that occur in samples produced according to the CAD model make it difficult to apply this solution.

Volumetric shrinkage rates calculated using equation 2 are presented in Table 2.

$$(A - B)/A \times 100 \tag{2}$$

where  $A$  is the CAD model volume and  $B$  is the as-printed and post-processed samples' volume.

As Table 2 shows, the volume of samples fabricated through 0.08 mm layer thickness is larger than the CAD model, while the volumes of the as-printed samples fabricated through 0.16 and 0.24 mm layer thickness are smaller. The effect of the 1 h VSF process on the material removal

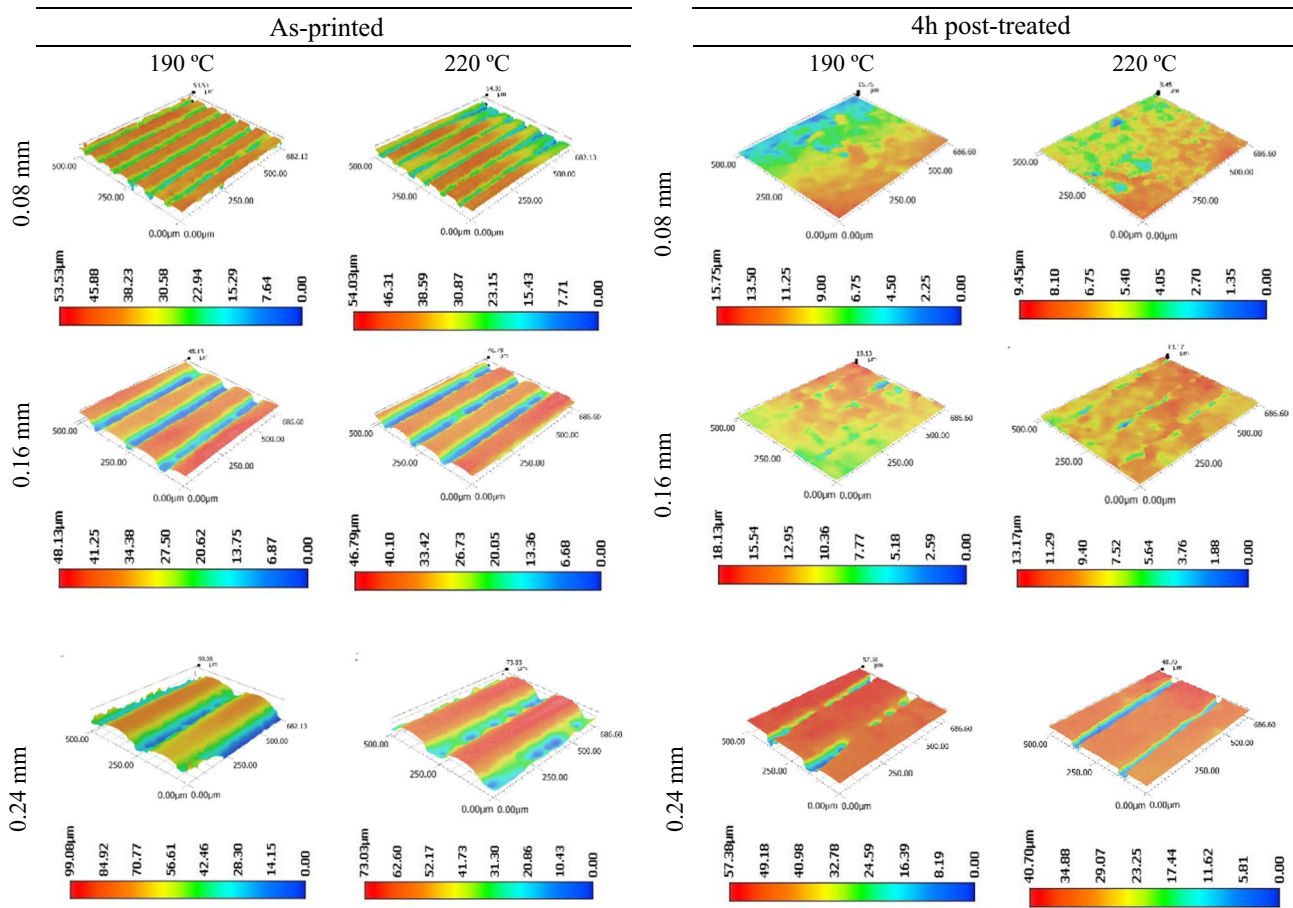


**Fig. 5** Surface topography images of samples after 4 h VSF process (built area)

rate (MRR) is evident. Because there was a decrease in volumes in all samples. Indeed, these results show agreement with the literature [23, 24, 34]. Due to the plasticity and diffusion process during extrusion of the filament, it tends to obtain the shape of an oval-like structure and will no longer be circular [35]. In building direction, oval-like filaments interact with each other and thus further dimensional inaccuracy and eventually distortion and volumetric shrinkage take place [35].

Another point needs to be discussed is the differences in the volumes of the same as-printed samples produced with different parameters. With the constant printing temperature, the increase in volume should be directly proportional to the increase in mass, since the density is considered constant. Figure 9 shows the effect of layer thickness on weight of material extrusion AM samples. The weight of the material extrusion AM samples increased with the increase in the layer thickness. It is possible to explain this situation with the volume of voids between two layers due to the stair casing effect. The profiles of the layers in the built area are shown in Fig. 10. The areas covered by the voids between peak and valleys and the number of voids number per unit

distance are not the same at each layer thickness. A heavier sample at 0.24 mm layer thickness and lighter sample at 0.08 mm layer thickness were produced in proportion to the distances between peak and valley  $h_3 > h_2 > h_1$ . In fact, the small layer thickness has the effect of increasing the cooling rate of the extruded filaments. While it is still possible to talk about the viscosity effect of PLA filaments, the viscosity effect should be greater as the increase in layer thickness will cause slower cooling. Thanks to the slower cooling, the voids at the junction points of the inner layers tend to decrease compared to the outermost layers. In this case, it is reflected in the mass and volume values of the part. However, the higher the layer thickness, the less expected part weight. This can probably be explained by the fact that thicker layers contain more voids and are therefore less dense. However, the fact that 40% of the infill density was chosen has a share in the emergence of a weight trend beyond the expected [36]. It should be also noted that an increase in  $hc$  leads to an increase in print speed [36]. Thus, the filament expanded and led to a decrease in the voids in the junction areas between the layers. This explains the increase in weight.

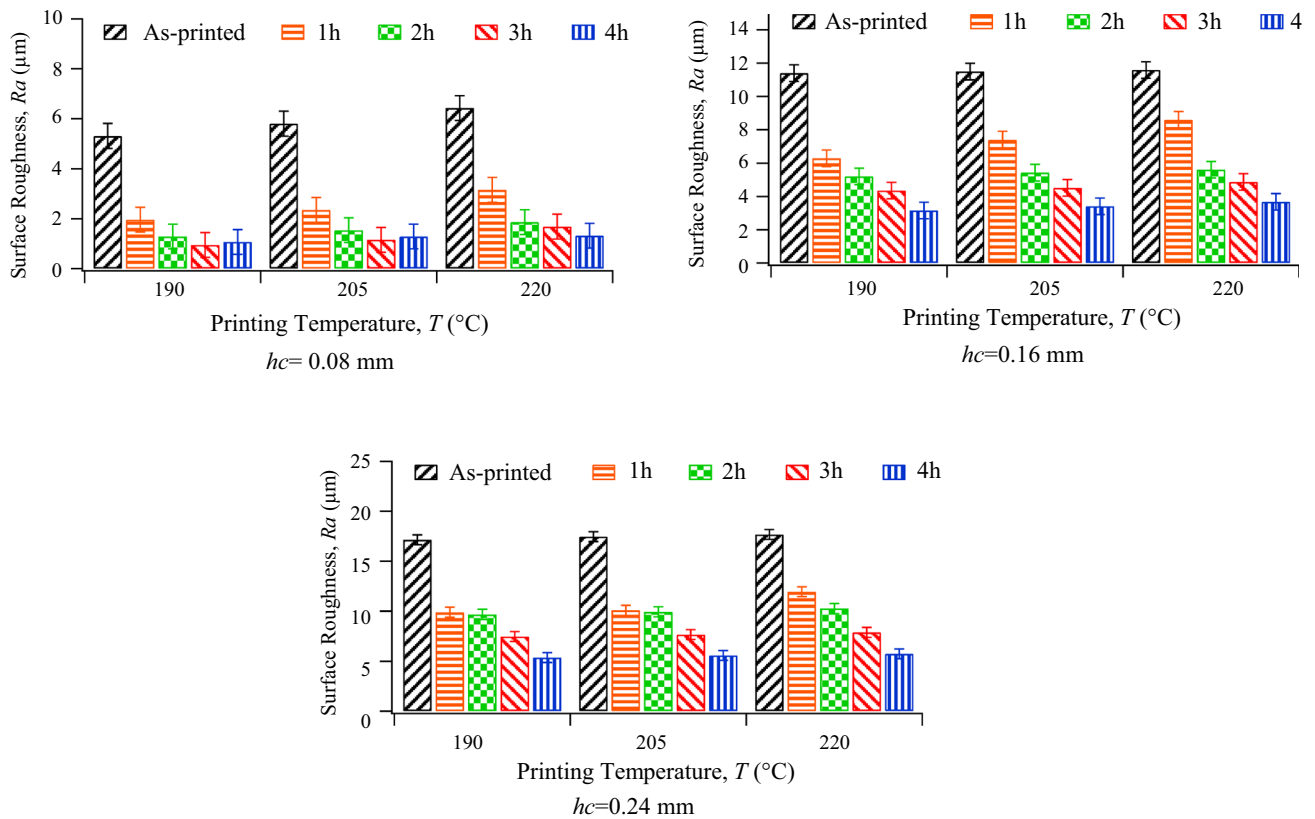


**Fig. 6** Measured average surface roughness on the built-area of as-printed and post-treated samples with various layer thickness

As-printed samples have large dimensional deviations considering the nominal dimensions of samples as shown in Fig. 11. While the samples fabricated with 0.16 and 0.24 mm layer thickness are larger than the nominal dimensions, samples fabricated with 0.08 mm layer thickness show variation with printing temperature. The role of printing temperature to dimensional deviation shows good agreement with the literature [37]. When printing temperature is raised, fluidity of filaments is also increased and produced layer is eventually expanded [38]. Figure 11 also confirms that post-processing operation makes remarkable changes on the dimension of samples fabricated by material extrusion process. Deviations are below the nominal value at 0.08 mm layer thickness and all VSF durations at 190 °C, and above the nominal value at 220 °C. In addition, the amount of deviation after 3 h VSF treatment at 205 °C is only 0.005% and can be neglected. An error of 0.025% was measured at 190 °C and 4 h VSF, which is the closest value to the nominal value at layer thickness of 0.16 mm. As in the conditions with 0.16 mm layer thickness, the error rate was measured as 0.12% at 0.24 mm layer thickness. These results also provide evidence that the selected input variables to fabricate samples play major role on the controlling dimensional accuracy of the samples. But, it also confirms that parameters should be optimized to obtain dimensions that are close to nominal values.

Although dimensional deviations can be eliminated by input parameters and VSF, it can cause rounding of corners and edges of the part in VSF processing.

### 3.3 Statistical analysis

As it is presented in previous section of this study, input parameters have an effect on measured outputs. However, to quantitatively determine the influence of each input variables on measured outputs, statistical analysis is performed. Printing temperature, layer thickness and post-processing duration are considered as variables in developing of mathematical models for surface roughness. The correlation in between printing temperature and layer thickness and surface roughness of as-printed samples is obtained by multiple linear regression. A linear polynomial model is developed to control whether the surface roughness data represent a fitness characteristic as below:

For as-printed samples,

$$\text{Surface roughness} = x_0 + x_1A + x_2B + x_3C + \dots + \epsilon \tag{3}$$

where  $x_{1,2}$  and  $x_3$  are estimates of the process parameters and  $\epsilon$  is error. A standard commercial statistical software MINITAB was used to drive the models. For the following

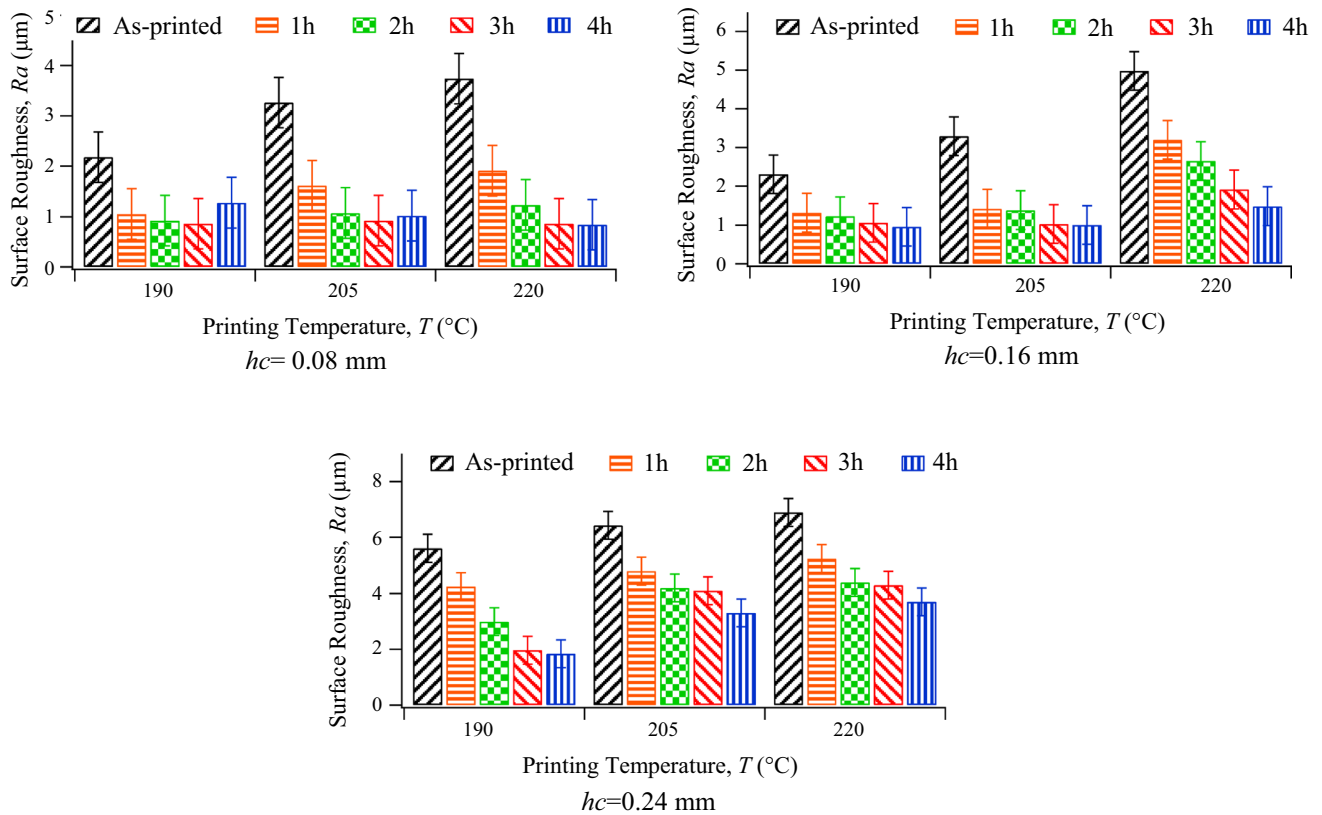


Fig. 7 Measured surface roughness on the scan-area of as printed and post-treated samples with various layer thickness

equations in between 4 and 9, *PT* indicates printing temperature, *hc* indicates layer thickness, *PPD* indicates post-process duration during vibratory surface finishing, *Dd* indicates dimensional deviation of as-printed samples, and *DdP* indicates dimensional deviation of post-processed samples.

As-Printed Parts' Average Surface Roughness:

$$Ra \text{ (Built Area)} = -4,18 + 72,38hc + 0,02042PT; R^2 = 99,8\% \tag{4}$$

$$Ra \text{ (Scan Area)} = -11,52 + 20,31hc + 0,0613PT; R^2 = 86,0\% \tag{5}$$

Post-treated Parts' Average Surface Roughness:

$$Ra \text{ (Built Area)} = -4,47 + 43,04hc + 0,0275PT - 0,01956PPD; R^2 = 94,3\% \tag{6}$$

$$Ra \text{ (Scan Area)} = -6,47 + 16,41hc + 0,03345PT - 0,00578PPD; R^2 = 79,3\% \tag{7}$$

As-Printed Parts' Dimensional Deviation:

$$Dd = -2,285 + 2,292hc + 0,01067PT; R^2 = 88,3\% \tag{8}$$

Post-treated Parts' Dimensional Deviation:

$$DdP = -2,421 + 2,122hc + 0,01150PT - 0,000876PPD; R^2 = 88,0\% \tag{9}$$

In multiple linear regression analysis,  $R^2$ , which is called as R-sq, is the regression coefficient ( $R^2 > 0.80$ ) for the models that indicate that the fit of the experimental data is satisfactory [39].

ANOVA helps in formally testing the significance of all main factors and their interactions by comparing the mean square against an estimate of the experimental errors at specific confidence levels. The details of ANOVA can be found in elsewhere[39]. Tables 3 and 4 show ANOVA results for surface roughness of as-printed samples considering their built area and scan area, respectively. It is obvious that layer thickness (*hc*) dominates the final surface roughness of samples in both directions, although it is likely the only parameter to determine surface quality in built area.

Tables 5 and 6 depict the effect of input variables including printing temperature, layer thickness and post-processing time on the measured average surface roughness of the samples. It is apparent that layer thickness is still determining the final surface quality after post-processing operation. The role of post-processing time also makes reasonable contributing for finalizing surface quality.

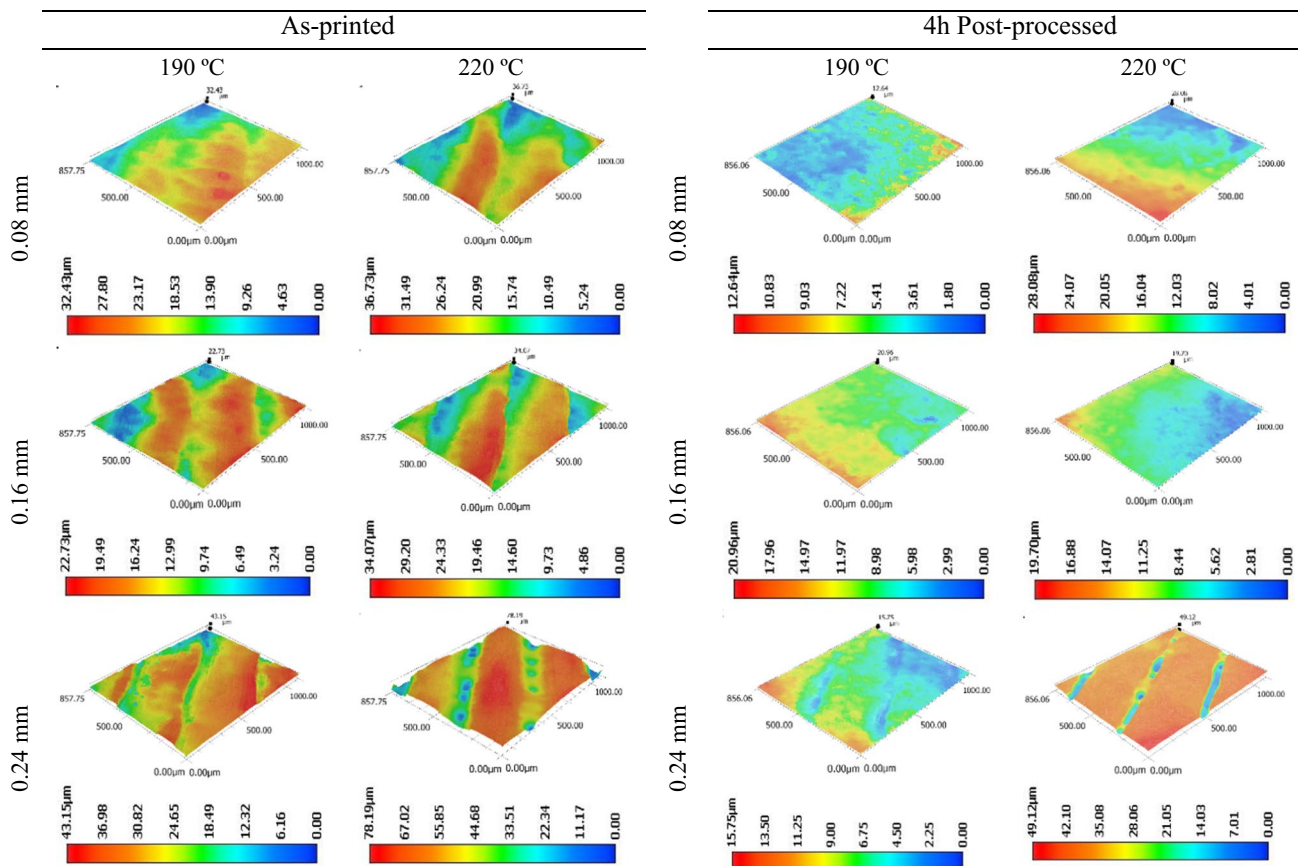


Fig. 8 Surface topography images of as-printed samples after 4 h VSF process (scan area)

Table 2 Volumetric shrinkage percentages of material extrusion AM as-printed and VSF samples

Layer thickness (mm)	Printing temperature (°C)	As-printed	1 h VSF
0.08	190	0.953	0.625
0.08	205	0.393	-0.116
0.08	220	0.291	-0.142
0.16	190	-0.012	-0.357
0.16	205	-0.186	-0.561
0.16	220	-0.655	-1.268
0.24	190	-0.222	-0.795
0.24	205	-0.632	-0.801
0.24	220	-0.744	-1.611

Tables 3 and 5 show that the p-value of PT is greater than alpha (0.05). In this case, it is concluded that the effect of PT on Ra is not significant. Therefore, it is a good approach to apply the pooling method in ANOVA analysis to ignore the effect of PT. In the pooling method, the non-significant factor is eliminated and the contribution of the remaining factors is highlighted [40]. Tables 7 and 8 show

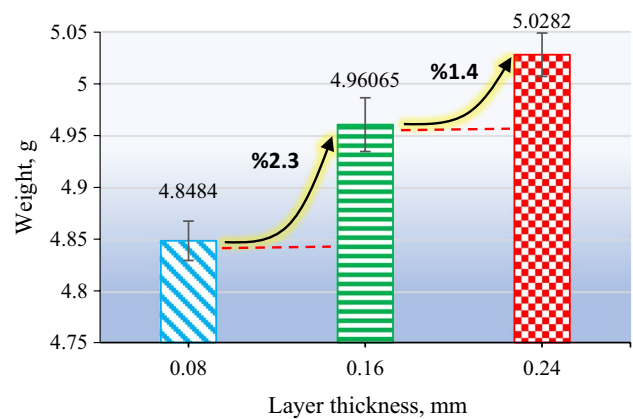


Fig. 9 Weights of the samples produced with various layer thickness and 205 °C constant printing temperature

the as-printed and post-treated samples' (built area) pooled ANOVA analysis.

Tables 9 and 10 show the role of input variables on dimensional deviation of as-printed and post-processed samples, respectively. Although in this case layer thickness has also major role on controlling dimensional deviation on the

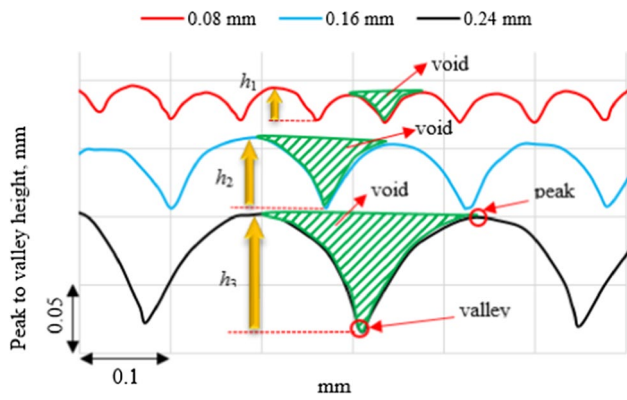


Fig. 10 Voids between layers at 205 °C constant printing temperature

printed samples, printing temperature is also a very effective parameter by contributing its variation by 38%. Considering dimensional variation after post-processing operation, printing temperature is a leading parameter among all three input variables. The role of post-treatment time is relatively limited to controlling dimensional deviation of samples, as shown in Table 10.

Statistical analysis also quantitatively confirms the significant input variables on both surface quality and dimensional variation of PLA specimens. The contribution of printing temperature within selected range is negligible for surface quality of samples, while to control dimensional accuracy, both printing temperature and layer thickness are significant

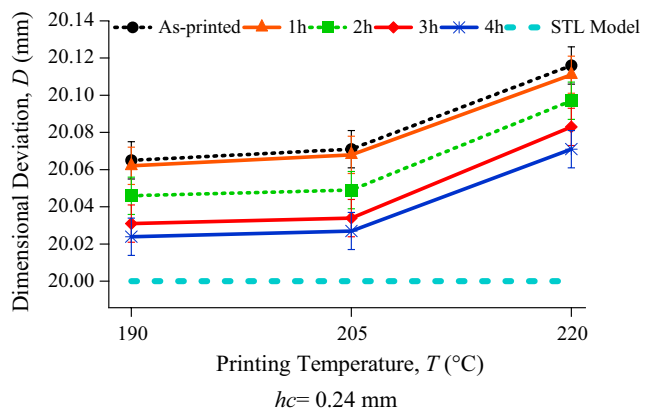
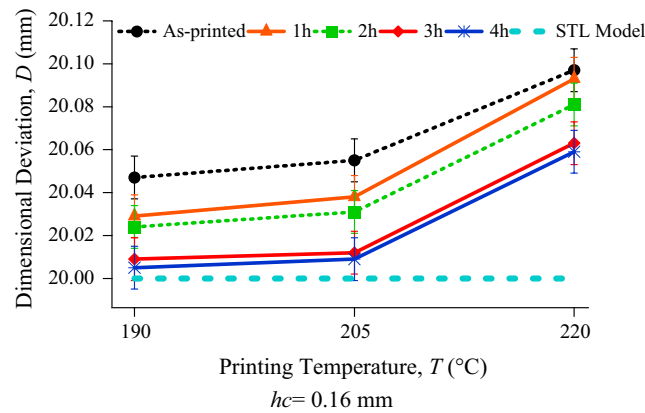
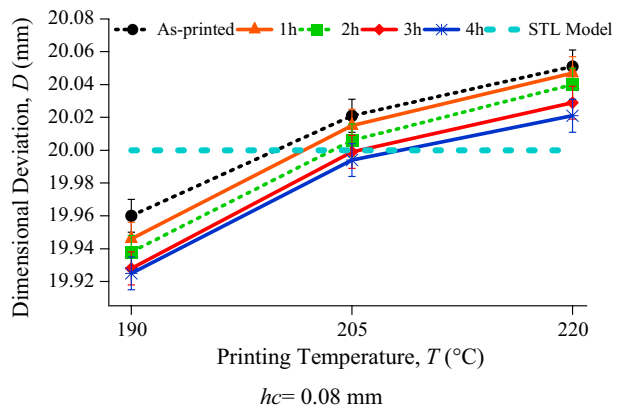
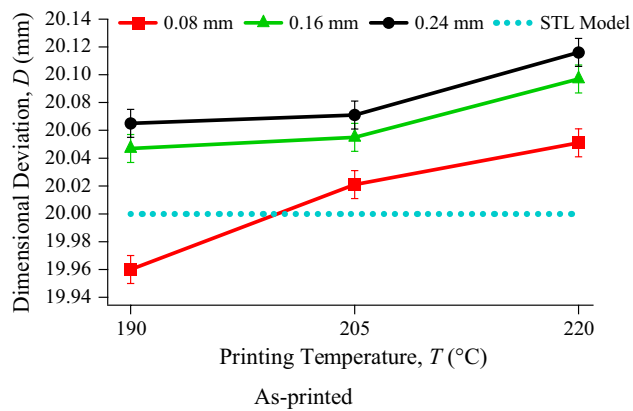


Fig. 11 Measured dimensional deviation of as-printed and post-treated samples fabricated by material extrusion AM

Table 3 ANOVA results for surface roughness of as-printed samples (built area)

Variance source	Degree of freedom (DOF)	Sum of squares (SS)	Mean square (MS)	F-ratio (F)	P-value (P)
hc	2	201.184	100.592	1826.12	0.000
PT	2	0.563	0.280	5.11	0.079
Error	4	0.220	0.055		
Total	4	201.967			

**Table 4** ANOVA results for surface roughness of as-printed samples (scan area)

Variance source	Degree of freedom (DOF)	Sum of squares (S)	Mean square (MS)	<i>F</i> -ratio ( <i>F</i> )	<i>P</i> -value ( <i>P</i> )	Percent (%)
<i>hc</i>	2	18.5180	9.2590	52.61	0.001	76.2
<i>PT</i>	2	5.0805	2.5402	14.43	0.015	20.9
Error	4	0.7039	0.1760			2.9
Total	8	24.3023				100

**Table 5** ANOVA results for surface roughness of post-treated samples (built area)

Variance source	Degree of freedom (DOF)	Sum of squares (S)	Mean square (MS)	<i>F</i> -ratio ( <i>F</i> )	<i>P</i> -value ( <i>P</i> )
<i>hc</i>	2	284.666	142.333	193.06	0.000
<i>PT</i>	2	4.113	2.056	2.79	0.079
<i>PPD</i>	3	62.083	20.694	28.07	0.000
Error	28	20.643	0.737		
Total	35	371.504			

**Table 6** ANOVA results for surface roughness of post-treated samples (scan area)

Variance source	Degree of freedom (DOF)	Sum of squares (S)	Mean Square (MS)	<i>F</i> -ratio ( <i>F</i> )	<i>P</i> -value ( <i>P</i> )	Percent (%)
<i>hc</i>	2	47.660	23.8299	93.17	0.000	71.62
<i>PT</i>	2	6.042	3.0210	11.81	0.000	9.08
<i>PPD</i>	3	5.678	1.8926	7.40	0.001	8.53
Error	28	7.161	0.2558			10.76
Total	35	66.541				100

**Table 7** Pooled ANOVA table for as-printed samples (built area)

Variance source	Degree of freedom (DOF)	Sum of squares (SS)	Mean square (MS)	<i>F</i> -ratio ( <i>F</i> )	<i>P</i> -value ( <i>P</i> )	Percent (%)
<i>hc</i>	2	201.184	100.592	770.38	0.000	99.62
Error	6	0.783	0.131			0.38
Total	4	201.967				100

**Table 8** Pooled ANOVA table for post-treated samples (built area)

Variance source	Degree of freedom (DOF)	Sum of squares (S)	Mean square (MS)	<i>F</i> -ratio ( <i>F</i> )	<i>P</i> -value ( <i>P</i> )	Percent (%)
<i>hc</i>	2	284.666	142.333	172.49	0.000	76.62
<i>PPD</i>	3	62.083	20.694	25.08	0.000	16.72
Error	30	24.755	0.825			6.66
Lack of fit	6	18.129	3.022	10.94	0.000	4.88
Pure Error	24	6.626	0.276			1.78
Total	35	371.504				100

**Table 9** ANOVA results for dimensional deviation of as-printed samples

Variance source	Degree of freedom (DOF)	Sum of squares (S)	Mean Square (MS)	<i>F</i> -ratio ( <i>F</i> )	<i>P</i> -value ( <i>P</i> )	Percent (%)
<i>hc</i>	2	0.21972	0.109858	16.66	0.011	54.63
<i>PT</i>	2	0.15605	0.078025	11.83	0.021	38.8
Error	4	0.02638	0.006596			6.56
Total	8	0.40215				100

**Table 10** ANOVA results for dimensional deviation of post-treated samples

Variance source	Degree of freedom (DOF)	Sum of squares (S)	Mean Square (MS)	<i>F</i> -ratio ( <i>F</i> )	<i>P</i> -value ( <i>P</i> )	Percent (%)
<i>hc</i>	2	0.7264	0.363177	64.38	0.000	41.76
<i>PT</i>	2	0.7278	0.363881	64.50	0.000	41.85
<i>PPD</i>	3	0.1270	0.042324	7.50	0.001	7.3
Error	28	0.1580	0.005641			9.08
Total	35	1.7391				100

that shows good agreement with the available literature, as mentioned in the previous section.

## 4 Conclusions

One of the major obstacles of material extrusion AM is poor surface and dimensional quality of fabricated parts. Considering industrial applications, this study focused on surface and dimensional quality of printed PLA samples by considering two main input variables that are printing temperature and layer thickness. Furthermore, vibratory surface finishing and duration of this operation are considered in terms of surface and dimensional accuracy of parts.

It is demonstrated that layer thickness is major player to determine surface quality of as-printed parts. Statistical results show that it affects surface roughness of as-printed and post-treated samples by 76.2 and 71.62%, respectively. The effect of printing temperature on surface roughness is not substantial. Statistical results confirm that it affects surface roughness of as-printed and post-treated samples by 20.9 and 9.08%, respectively. However, printing temperature is a critical parameter to control dimensional accuracy of printed parts. Statistical results show that it affects dimensional accuracy of as-printed and post-treated samples by 38.8 and 41.85%, respectively. The tested post-processing operation and its duration are also helpful to give the final form to the printed parts.

The current results demonstrated that preferring larger layer thickness to reduce production time and cost is reasonable option; but, it should be noted that larger layer thickness produces poor surface quality. However, depending on

the application, by using post-processing operation such as vibratory surface finishing is notable approach. It is also a method that can be used not only for PLA, but also for ABS and other polymer materials. This makes it possible to post-process many different materials with a single investment cost in industrial applications.

## Declarations

**Conflict of interest** The authors declare no competing interests.

## References

- Kumbhar N, Mulay A (2018) Post processing methods used to improve surface finish of products which are manufactured by additive manufacturing technologies: a review. *J Inst Eng (India) Series C* 99(4):481–487. <https://doi.org/10.1007/s40032-016-0340-z>
- ISO/ASTM52900–15 (2015) Standard terminology for additive manufacturing – general principles – terminology. ASTM International. West Conshohocken
- Galantucci LM, Lavecchia F, Percoco G (2009) Experimental study aiming to enhance the surface finish of fused deposition modeled parts. *CIRP Ann* 58(1):189–192. <https://doi.org/10.1016/j.cirp.2009.03.071>
- Turner BN, Gold SA (2015) A review of melt extrusion additive manufacturing processes: II. Materials, dimensional accuracy, and surface roughness. *Rapid Prototyping J*. <https://doi.org/10.1108/RPJ-02-2013-0017>
- Messimer SL, Patterson AE, Muna N, Deshpande AP, Rocha Pereira T (2018) Characterization and processing behavior of heated aluminum-polycarbonate composite build plates for the

- FDM additive manufacturing process. *J Manuf Mater Process* 2(1):12. <https://doi.org/10.3390/jmmp2010012>
6. Rodríguez-Panes A, Claver J, Camacho AM (2018) The influence of manufacturing parameters on the mechanical behaviour of PLA and ABS pieces manufactured by FDM: a comparative analysis. *Materials* 11(8):1333. <https://doi.org/10.3390/ma11081333>
  7. Casavola C, Cazzato A, Moramarco V, Pappalettera G (2017) Preliminary study on residual stress in FDM parts. In: *Residual stress, thermomechanics & infrared imaging, hybrid techniques and inverse problems*, Volume 9. Springer, pp 91–96. [https://doi.org/10.1007/978-3-319-42255-8\\_12](https://doi.org/10.1007/978-3-319-42255-8_12)
  8. Chen Y, Geever LM, Killion JA, Lyons JG, Higginbotham CL, Devine DM (2016) Review of multifarious applications of poly (lactic acid). *Polym-Plast Technol Eng* 55(10):1057–1075. <https://doi.org/10.1080/03602559.2015.1132465>
  9. Bouzouita A, Notta-Cuvier D, Raquez J-M, Lauro F, Dubois P (2017) Poly (lactic acid)-based materials for automotive applications. *Ind Appl Poly (lactic acid)*. [https://doi.org/10.1007/12\\_2017\\_10](https://doi.org/10.1007/12_2017_10)
  10. Thompson MK, Moroni G, Vaneker T, Fadel G, Campbell RL, Gibson I, Bernard A, Schulz J, Graf P, Ahuja B (2016) Design for Additive Manufacturing: trends, opportunities, considerations, and constraints. *CIRP Ann* 65(2):737–760. <https://doi.org/10.1016/j.cirp.2016.05.004>
  11. Chohan JS, Singh R (2017) Pre and post processing techniques to improve surface characteristics of FDM parts: a state of art review and future applications. *Rapid Prototyping J*. <https://doi.org/10.1108/RPJ-05-2015-0059>
  12. Kovan V, Tezel T, Topal E, Camurlu H (2018) Printing parameters effect on surface characteristics of 3D printed PLA materials. *Mach Technol Mater* 12(7):266–269
  13. Rajpurohit SR, Dave HK (2018) Effect of process parameters on tensile strength of FDM printed PLA part. *Rapid Prototyping J*. <https://doi.org/10.1108/RPJ-06-2017-0134>
  14. Wankhede V, Jagetiya D, Joshi A, Chaudhari R (2020) Experimental investigation of FDM process parameters using Taguchi analysis. *Mater Today Proc* 27:2117–2120. <https://doi.org/10.1016/j.matpr.2019.09.078>
  15. Vijay P, Danaiah P, Rajesh K (2011) Critical parameters effecting the rapid prototyping surface finish. *J Mech Eng Autom* 1(1):17–20
  16. Pugalendhi S (2012) Experimental investigation of surface roughness for fused deposition modelled part with different angular orientation. *ADMT J* 5(3):21–28
  17. Rayegani F, Onwubolu GC (2014) Fused deposition modelling (FDM) process parameter prediction and optimization using group method for data handling (GMDH) and differential evolution (DE). *The Int J Adv Manuf Technol* 73(1–4):509–519. <https://doi.org/10.1007/s00170-014-5835-2>
  18. Campbell RI, Martorelli M, Lee HS (2002) Surface roughness visualisation for rapid prototyping models. *Comput Aided Des* 34(10):717–725. [https://doi.org/10.1016/S0010-4485\(01\)00201-9](https://doi.org/10.1016/S0010-4485(01)00201-9)
  19. Boschetto A, Bottini L (2015) Roughness prediction in coupled operations of fused deposition modeling and barrel finishing. *J Mater Process Technol* 219:181–192. <https://doi.org/10.1016/j.jmatprotec.2014.12.021>
  20. Singh R, Trivedi A (2017) Experimental investigations for surface roughness and dimensional accuracy of FDM components with barrel finishing. *Proc Natl Acad Sci India Sect A* 87(3):455–463. <https://doi.org/10.1007/s40010-017-0367-4>
  21. Jamal M, Morgan M (2017) Design process control for improved surface finish of metal additive manufactured parts of complex build geometry. *Inventions* 2(4):36. <https://doi.org/10.3390/inventions2040036>
  22. Delfs PZ, Li H (2015) Schmid mass finishing of laser sintered parts. In: *Proceedings of the 26th annual international solid freeform fabrication symposium*
  23. Schmid M, Simon C, Levy G (2009) Finishing of SLS-parts for rapid manufacturing (RM)—a comprehensive approach. *Proceedings SFF*:1–10. <https://doi.org/10.26153/tsw/15081>
  24. Fischer MV (2013) Schöppner some investigations regarding the surface treatment of Ultem\* 9085 parts manufactured with fused deposition modeling. In: *24th annual international solid freeform fabrication symposium, Austin*, pp 12–14
  25. Ultimaker Tough PLA Technical Data Sheet. <https://support.ultimaker.com/hc/en-us/articles/360012759599-Ultimaker-Tough-PLA-TDS>. Accessed 04.02.2022
  26. Ultimaker Ultimaker S5 Pro PDF manuals. <https://support.ultimaker.com/hc/en-us/articles/360013034239-Ultimaker-S5-Pro-Bundle-PDF-manuals>. Accessed 04.02.2022
  27. Yang L, Li S, Li Y, Yang M, Yuan Q (2019) Experimental investigations for optimizing the extrusion parameters on FDM PLA printed parts. *J Mater Eng Perform* 28(1):169–182. <https://doi.org/10.1007/s11665-018-3784-x>
  28. Moradi M, Aminzadeh A, Rahmatbadi D, Hakimi A (2021) Experimental investigation on mechanical characterization of 3D printed PLA produced by fused deposition modeling (FDM). *Mater Res Expr* 8(3):035304
  29. Pérez CL, Calvet JV, Pérez MS (2001) Geometric roughness analysis in solid free-form manufacturing processes. *J Mater Process Technol* 119(1–3):52–57. [https://doi.org/10.1016/S0924-0136\(01\)00897-4](https://doi.org/10.1016/S0924-0136(01)00897-4)
  30. Bakar NSA, Alkahari MR, Boejang H (2010) Analysis on fused deposition modelling performance. *J Zhejiang Univ Sci A* 11(12):972–977. <https://doi.org/10.1631/jzus.A1001365>
  31. Alsoufi MS, Elsayed AE (2017) How surface roughness performance of printed parts manufactured by desktop FDM 3D printer with PLA+ is influenced by measuring direction. *Am J Mech Eng* 5(5):211–222
  32. Byun H-S, Lee KH (2003) Design of a new test part for benchmarking the accuracy and surface finish of rapid prototyping processes. In: *International conference on computational science and its applications*, Springer, pp 731–740. [https://doi.org/10.1007/3-540-44842-X\\_74](https://doi.org/10.1007/3-540-44842-X_74)
  33. Xu F, Loh H, Wong Y (1999) Considerations and selection of optimal orientation for different rapid prototyping systems. *Rapid Prototyping J*. <https://doi.org/10.1108/13552549910267344>
  34. Fischer M, Schöppner V (2014) Finishing of ABS-M30 parts manufactured with fused deposition modeling with focus on dimensional accuracy. In: *Proceedings of 25th solid freeform fabrication symposium*, pp 923–934
  35. Gurralla PK, Regalla SP (2014) Multi-objective optimisation of strength and volumetric shrinkage of FDM parts: a multi-objective optimization scheme is used to optimize the strength and volumetric shrinkage of FDM parts considering different process parameters. *Virtual Phys Prototyping* 9(2):127–138. <https://doi.org/10.1080/17452759.2014.898851>
  36. Peng AH, Wang ZM (2010) Researches into influence of process parameters on FDM parts precision. *Appl Mech Mater*. <https://doi.org/10.4028/www.scientific.net/AMM.34-35.338>
  37. Valerga AP, Batista M, Salguero J, Girot F (2018) Influence of PLA filament conditions on characteristics of FDM parts. *Materials* 11(8):1322. <https://doi.org/10.3390/ma11081322>
  38. Valerga A, Batista M, Puyana R, Sambruno A, Wendt C, Marcos M (2017) Preliminary study of PLA wire colour effects on

- geometric characteristics of parts manufactured by FDM. *Procedia Manuf* 13:924–931. <https://doi.org/10.1016/j.promfg.2017.09.161>
39. Kurt M, Kaynak Y, Bagci E, Demirer H, Kurt M (2009) Dimensional analyses and surface quality of the laser cutting process for engineering plastics. *The Int J Adv Manuf Technol* 41(3–4):259–267. <https://doi.org/10.1007/s00170-008-1468-7>
40. Ibrahim MM, Sia C, Ahmad Z (2002) Preliminary step in formulating the optimum electroless nickel bath using Taguchi method. *Jurnal Teknologi*:67â€“74–67â€“74

**Publisher's Note** Springer Nature remains neutral with regard to jurisdictional claims in published maps and institutional affiliations.